International Journal of Thermal Sciences 48 (2009) 2264–2270

Contents lists available at ScienceDirect

International Journal of Thermal Sciences

journal homepage: www.elsevier.com/locate/ijts

Neural network based correlation for critical heat flux in steam-water flows in pipes

Ahmed Safwat Nafey

Department of Engineering Science, Faculty of Petroleum and Mining Engineering, Suez Canal University, Suez, Egypt

ARTICLE INFO

Article history:
Received 19 June 2007
Received in revised form
11 April 2009
Accepted 27 April 2009
Available online 3 June 2009

Keywords:
Artificial neural network (ANN)
Critical heat flux
ANN based correlation
Steam–water mixture flow

ABSTRACT

This paper presents a new approach using artificial neural networks (ANN) to predict the critical heat flux (CHF) for a steam–water mixture through pipes. A large number of experimental measurements are used for training and testing the developed network. The Levenberg–Marquardt algorithm was used to train the developed feed forward ANN. The training and validation are performed with good accuracy. The correlation coefficient obtained with unknown data applied to the network is 0.998 which is satisfactory and verifying the fidelity of the developed network. The present methodology proved to be much better than the traditional table and best-fit methods. Using the weights and biases obtained from the trained network, a new formulation is proposed for determination of the CHF Q_{cr}. Experimental results of Q_{cr} are compared with both the results obtained by the developed ANN based correlation and the results obtained by a best-fit correlation. Deviations between the results are found to be less than 5.5% and 30%, respectively. The developed ANN based correlation may make use of the dedicated ANN software unnecessary to use for each calculation time. As seen from the results obtained, the calculated Q_{cr} is obviously within acceptable uncertainties. This ANN based correlation can be employed with any programming language or spreadsheet program for estimating the CHF Q_{cr}. If the validity range changes, the ANN based correlation can be updated in terms of new sets of weights and biases using the same network architecture (same no. of hidden layers and no. of neurons).

1. Introduction

The critical heat flux (CHF) is a limiting factor for most forced convective boiling processes. CHF refers to the heat transfer limit causing a sudden decrease in the heat transfer coefficient and possible catastrophic failure of the device in which evaporation or boiling is occurring. For a heat flux-controlled system, exceeding the CHF can lead to a sudden large increase in the wall temperature, which for most coolants, can lead to system failure. The capability to predict the CHF is therefore of vital importance to the safety of flow boiling process [1]. The CHF prediction in the boiling heat transfer equipments could be useful to know the real causes of the failures presented, like the burnout of tubes or leaks that appear as consequence of an accelerated process of corrosion caused by the high temperature reached in the material. However, CHF is one of the most studied and least understood phenomenon in flow boiling. Over 500 prediction methods for CHF exist in the literature. The increase of CHF prediction methods indicates the lack of understanding of CHF, and makes it difficult to choose a suitable CHF prediction method or correlation. Therefore, predicting CHF is a very challenging task.

A considerable amount of information has been presented concerning the CHF for different fluids flowing through round tubes [1–8]. Various authors have established different techniques and different relationships for CHF prediction. The quantitative relationship between the main variables, however, varies from one author to another. One could wonder whether such forms, both so unlike and involving different sets of input variables, could accurately represent the same heat transfer phenomenon. This evident discrepancy is reasonably due to the different approaches in evaluating the essential elements composing the initial tentative model from which to start the functional form development.

In general, the CHF prediction can be realized in two main different ways: collecting data into a multidimensional table (table method) or creating a best-fit correlation (best-fit method) as a function of the main parameters. The best-fit method based on assuming a correlation form consists of combination of non-dimensional numbers, which characterize some phenomenological processes, and in fitting some adjustment coefficients. The fitting process may be rather complex for fluids. The CHF look-up tables [9,10] and extensive set of correlation packages [1] are good

E-mail address: asnafey31@yahoo.com

1290-0729/$ – see front matter © 2009 Published by Elsevier Masson SAS.
doi:10.1016/j.ijthermalsci.2009.04.010

Nomenclature

d	Diameter of the tube (mm), desired output (target)
g	Mass flow rate $\mathrm{kg\,m^{-2}\,s^{-1}}$
k	Number of neurons in hidden layer
l	Heated length (mm)
M	Number of input parameters
N	Number of learning data
p	Pressure (kPa)
Q_{cr}	Critical heat flux ($\mathrm{kW\,m^{-2}}$)
t	Temperature (°C)
w	Weight
w_{ji}	Weight between the neurons j and i
x	Vapor fraction (quality) at the outlet of the pipe
ν', ν''	Specific gravity of the liquid and saturated vapor, respectively

examples for the first and second methods, respectively. Tong and Tang [1] evaluated these two methods as follows: in one hand, the Groeneveld CHF look-up table predicts the general trend of pressure p, fluid mass velocity g, steam quality by weight x, water temperature entering t, length l, and diameter d effects well. However, to apply the table method to reactor design, proper adjustments for detailed geometrical effects of a prototype rod bundle would be needed. Such adjustments are usually expressed in empirical formulae that are as complicated as the existing CHF design correlations. Thus, in this case the table method does not provide much more convenience. Indeed, the table method requires an interpolator and a difficult preliminary work of point selection and smoothing in order to avoid meaningless irregularities induced by the data scattering. On the other hand, the CHF prediction correlations have been developed assuming an initial tentative model, which undergoes successive modifications to correct discrepancies with respect to experimental results using a "trial-and-error" approach. Depending on the initial structure of the tentative model and on the criteria of the subsequent modifications the resulting correlations proposed in the literature often present a formulism quite different from the other. In general, a CHF correlation is accurate only in the particular flow regimes within the ranges of the operating parameters in which it was developed. Consequently, the application of CHF correlation should be limited to within these ranges of parameters. A universal correlation has not yet been developed up to now.

Modern computational capabilities and numerical optimization techniques would make the table and best-fit methods somewhat out of use. Recently, artificial neural network (ANN) (as one of artificial intelligence techniques) is widely accepted as a technology offering an alternative way to tackle complex and ill-defined problems. ANN technique has a number of advantages such as; fault tolerant in the sense that it is able to handle noisy and incomplete data. ANN can learn from examples, and deal with non-linear problems. Also, ANN has large degree of freedom, ease of use (no fluid properties are needed) ease of updating and accurate predictin at very high speed. ANN are systems of weight and biases vectors, whose component values are established through various machine-learning algorithms, which take as input a linear set of pattern inputs and produce as output a numerical pattern representing the actual output. ANNs mimic somewhat the learning process of a human brain. Instead of complex rules and mathematical routines, ANNs are able to learn key information patterns within a multi-information domain. ANNs differ from the traditional modeling approaches in that they are trained to learn solutions rather than being programmed to model a specific problem in the normal way [11].

ANN has been applied successfully in various fields of mathematics, medicine, economics, meteorology, psychology, neurology, and many others. ANNs have been used in many engineering applications such as in control systems, in classification, and in modeling complex process transformations [11–14,15].

The ANN methodology enables us to design useful nonlinear systems accepting large numbers of input, with the design based solely on instances of input–output relationships and has proved that it is a very powerful and efficient tool to analyze different heat transfer processes. Thus, ANN can be used as a predictor of CHF based on the available database without knowing their best-fit correlations due to ANN's black-box characteristic. However, although the ANNs can perform quite well for interpolation between patterns that have been used during the learning phase, they are poor in extrapolating. Thus, one has to strive to collect experimental data as much as possible in order to train the ANN in which all parameters that have effects on CHF will be considered within a wide parameter range.

It is important to note that if the validity range changes, development of traditional correlations such as Eq. (1) [16] will require much effort. Updating of the constant coefficients of the correlation may not be sufficient and structure of the correlation may be altered altogether. However, ANN based correlation can be updated in terms of new sets of weights and biases using the same architecture (same no. of hidden layers and no. of neurons) reliably with new plant data by training, validation, and testing using the plant automation software.

$$Q_{cr} = 40(g)^n(1-x)^m\left(\frac{\nu'}{\nu''}\right)^{2.2}\left[1+\frac{8\times10^9}{(g)^{\mathrm{h}}}\right]\left[\mathrm{k\ cal/m^2\ h}\right] \quad (1)$$

where

$$n = 0.56 - 0.0189\frac{\nu'}{\nu''}$$

$$m = 0.7\frac{\nu'}{\nu''} - 0.4$$

$$h = 1.13 + 3.6\frac{\nu''}{\nu'} - 0.45x$$

In this study, the artificial neural networks approach is applied to develop an ANN based correlation for estimating the CHF (Q_{cr}) ($\mathrm{kcal/m^2\,h}$) for flow of steam–water mixtures (saturated poling conditions) through pipes for given outlet pressure p (atm), entering water temperature t (°C), steam quality by weight x, mass velocity of the steam–water mixture g ($\mathrm{kg/m^2\,h}$), pipe length l (mm), wall thickness δ (mm), and the pipe diameter d (mm). The output is the Q_{cr} of the flowing water–steam mixture. The ultimate objective is to use this correlation within the boiling heat transfer equipment modeling and optimization framework in the future.

2. Artificial neural networks approach

Neural networks operate much as a "black-box" model requiring no detailed information about the system. On the other hand, they learn the relationship between the input and the target. The network usually consists of an input layer, some hidden layers, and output layer. For a given set of inputs, ANNs are able to produce a corresponding set of outputs according to some mapping relationships. These relationships are encoded into the network structure during the training process (also called learning), and are dependant upon the parameters of the network, i.e. weights and biases which are iteratively adjusted in order to produce the nearest output to the desired target (experimental data) of the network [17].

Among the various kinds of ANNs that exist, the feed forward neural network has become the most popular in engineering applications [17], and it is the type being used in this article. The network is somewhat simple in structure and easily mathematically analyzed. The back propagation (BP) technique is the first and most commonly used feed forward neural network because of its mathematical strict learning scheme to train the network and guarantee mapping between inputs and outputs [18]. ANNs consisting of very simple and highly interconnected processors called neuron. These processors are analogous to biological neurons in human brain. A typical feed forward architecture is schematically illustrated in Fig. 1. This configuration has one input layer, one hidden layer and one output layer. During the feed forward stage, a set of input data is supplied to the input nodes (neurons) and the information is transferred forward through the network to the nodes in the output layer. The nodes perform non-linear input–output transformations by means of selected activation functions. The mathematical background, the procedures for training and testing the ANNs, and account of its history can be found in a text by Haykin [18]. The neurons are connected to each other by weighted links over which signals can pass. Each neuron receives multiple inputs from other neurons in proportion to their connection weights and biases and generates a single output, which may be propagated to several other neurons [19–20]. The non-linear mapping capability and the fact that the neurons are massively connected enable the ANNs to estimate any function without the need of an explicit mathematical model of the physical phenomenon.

Each neuron j in the ith layer (except in the input layer) is connected with all the neurons of the $(i-1)$-th layer with a bias (b_j^i) and through weights (w_{jk}^i). k denotes the neuron of $(ii-1)$-th layer. The total number of neurons in layer i is nj and the transfer function for layer i and neuron j is f_j^i. In each layer, the value of the neuron j is calculated by:

$$a_j^i = f_j^i\left(\sum_{k=1}^{n_{i-1}} w_{jk}^i \times a_k^{i-1} + b_j^i\right) \tag{2}$$

or

$$a_j^i = f_j^i\left(Z_j^i\right) \tag{3}$$

2.1. ANN architecture

The architecture of a neural network gives the description of the suitable number of layers which the network has, the number of neurons in each layer, the transfer function used in each layer, and how the layers are connected to each other. Each input is multiplied by a connection weight. In the simplest case, the products and biases are simply summed, then transferred through a transfer function to generate a result and finally, the output is obtained. Networks with biases can represent relationships between input and outputs more easily than networks without biases [18].

The configuration of the ANN is set by selecting the number of hidden layers and the number of nodes in these hidden layers, since the number of nodes in the input and output layers is determined from physical variables. In fact, the capability of three-layer network to approximate any continuous function has been proved [21,22]. Furthermore, the greater number of hidden layers, the more error transfers steps, which lead of course to the decrease of the generalization. So, this study first considers three-layer networks (one hidden layer). In selecting the optimum network parameters (learning rate, momentum coefficient, neuron number in hidden layer and iteration number). The program looks for the conditions where the root-mean square error (Eq. (4)) is minimum. During the learning, the error is estimated by mean square error (MSE) and the correlation coefficient (R^2) is defined as follows:

$$\mathrm{MSE} = \left(\frac{1}{n}\sum_j \left|t_j - p_j\right|^2\right)^{1/2} \tag{4}$$

$$R^2 = 1 - \left(\frac{\sum_j \left(t_j - p_j\right)^2}{\sum_j \left(p_j\right)^2}\right) \tag{5}$$

where t is the target (actual) value, p is the output (predictive) value and n is the number of patterns.

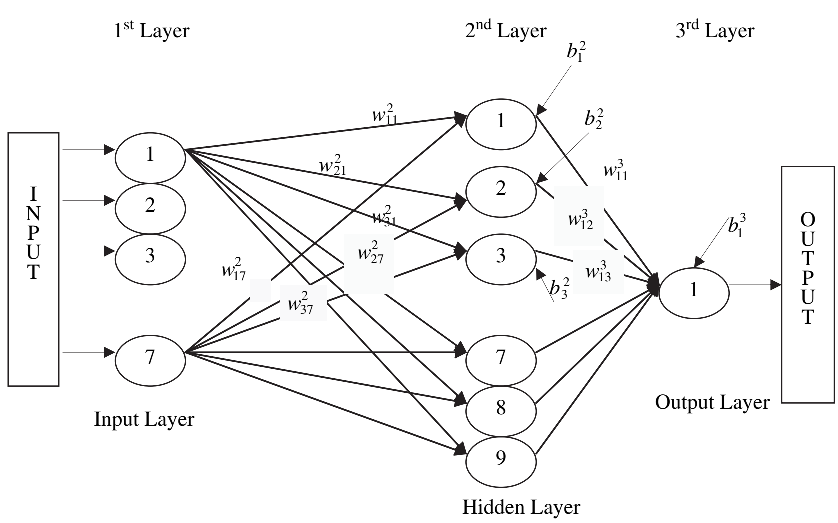

Fig. 1. Typical feed forward ANN architecture.

To determine the optimum network parameters, the learning rate (the rate at which the network learns) and momentum coefficient values are examined. The momentum coefficient is used to allow the network to avoid setting in local minima error (root-mean square error, MSE). Local minima in the MSE do not represent the best set of weight and bias factors and the global minimum does. Also, the neuron number in the hidden layer is tested between 2 and 12 and mean square error is calculated for each of them. After many trials optimum network parameters are found; the learning rate is 0.75 and momentum coefficient is 0.85 and the neuron number at hidden layer is 9. Therefore, the configuration 7–9–1 appeared to be the most optimal topology for this application.

2.2. Training algorithm

There are different learning algorithms. A popular algorithm is the back propagation (BP) algorithm [23], which has different variants. Standard back propagation is a gradient descent algorithm. It is very difficult to know which training algorithm will be the fastest for a given problem. By comparison, TRAINBR is found to be the best training algorithm in this case. Details about the algorithm can be seen in the help files of MATLAB 7.0 [23]. An ANN with a back propagation algorithm learns by changing iteratively the weights, and biases. These changes are stored as perception information, or knowledge.

The iteration process is ended at one of the following three conditions: (a) training error reaches an expected value such as 0.00001; (b) gradient reaches the minimal value; (c) number of iteration reaches a set value such as 3000.

2.3. Transfer functions

A transfer function generally consists of either linear or nonlinear algebraic equation [24]. There are three kinds of popular transfer functions which can be used in BP network: log-sig, tan-sig, and pure line. ANN models with hidden and output layers using different combinations of the three transfer functions are investigated in this work. The logistic sigmoid (log-sig) (Eq. (6)) and pure line (Eq. (7)) are used as model's hidden and output transfer functions, respectively.

$$f(Z) = \frac{1}{1+e^{-Z}}, \quad 0 \le f(Z) \le 1 \tag{6}$$

$$f(Z) = Z \tag{7}$$

where Z is the weighted sum and biases of input (Eq. (3))

2.4. Experimental input and output data

Experimental data for critical heat flux (Q_{cr}) for steam–water mixtures flowing in tubes with $250 \le l \le 3000$ mm in length, inside diameter $8 \le d \le 10$ mm, and wall thickness $0.75 \le \delta \le 1$ mm at pressures $100 \le p \le 200$ atm, mass velocity $3 \times 10^6 \le g \le 18 \times 10^6$ $\mathrm{kg_m/m^2\,h}$ and steam qualities (by weight) $0 \le x \le 40\%$ are used in this work [16]. The correlation (1) is selected in this work because it was developed by Peskov et al. [16] based on the same experimental data used in this study. Peskov shows that the error for 679 of the point's relative error to the correlation is between 0 and ±15%. And the error for the remaining 136 points is between ±15% and ±25%. Two subsets of data are used to build the ANN model: a training set and a testing set. In order to develop a formulation procedure for CHF (Q_{cr}) of steam–water mixtures flowing in tubes using ANNs, the training data set are selected in such a way that it includes the data from all regions of a desirable operation.

2.5. ANN training and testing

An important stage of a neural network is the training step, in which an input is introduced to the network together with the desired target; the weights and biases are adjusted iteratively so that the network attempts to produce the desired output. Calculating the error between the output and the target performs this process. This error is fed back to the network with adjusting weights and biases according to least mean square error (MSE) criteria. The process is continued until the network output is close to the target. The weights and biases, after training, contain meaningful information, whereas before training, they are random and have no meaning. When a satisfactory level of performance is reached, the training stops, and the network use the weights and biases to make decision. A suitably trained and validated network should be able to predict realistic output even when the network is simulated with new inputs (test data). The decrease of the mean square error (MSE) during the training process of the selected topology is shown in Fig. 2. The regression curve of the output variable Q_{cr} for the training data set is shown in Fig. 3. The correction coefficient obtained in this case is 0.999, which is very satisfactory.

2.6. Verification of the ANN

After the training session, the network was simulated with the test data. The regression curve of the output variable (Q_{cr}) for the test data set is shown in Fig. 4. It should be noted that these data were completely unknown to the network. The correlation coefficient obtained is 0.998, which is very satisfactory. In Table 1, a comparison is presented between the actual (experimental) Q_{cr} and the critical heat flux obtained by using both the developed ANN based correlation (illustrated in the next section) and best-fit correlation (Eq. (1)). As can be seen, the ANN based correlation percentage error is much better than the values produced by the correlation (1). The relative error is defined as:

$$Q_{error} = \frac{Q_{ANN} - Q_{EXP}}{Q_{EXP}} \times 100\% \tag{8}$$

where Q_{ANN} is the value of Q_{cr} obtained by ANN based correlation, and Q_{EXP} is the experimental value of Q_{cr}.

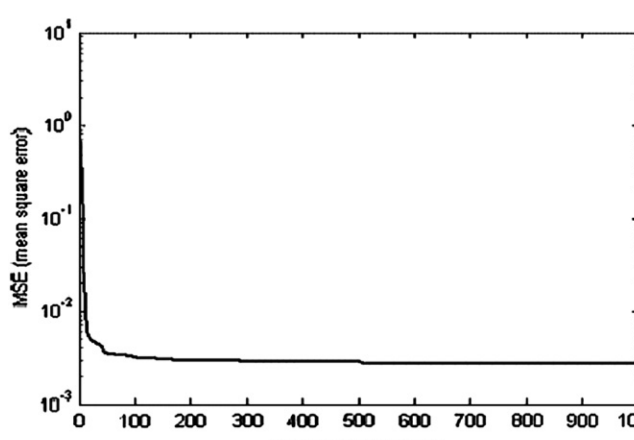

Fig. 2. Training result based on the (7–9–1) configuration.

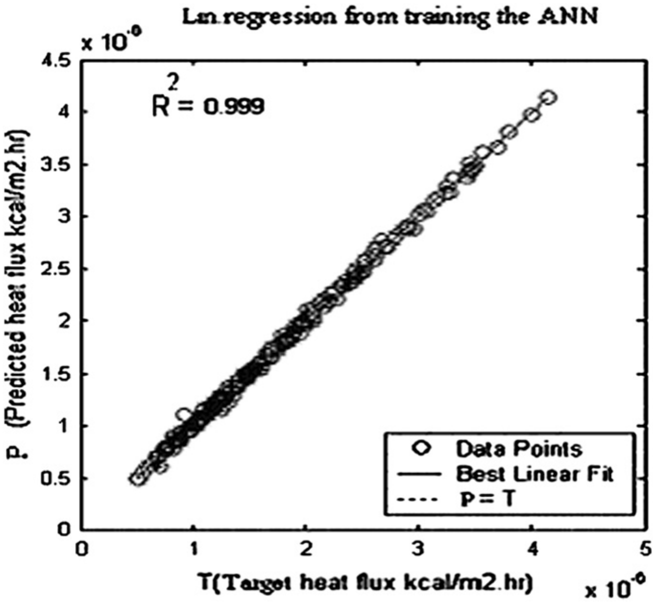

Fig. 3. Comparison of target and ANN-predicted values for critical heat flux (from training process).

Mathematical formulation can now be derived from the resulting weights, biases and the activation functions used in the ANN. As the regression coefficients obtained from both the training and testing of the ANNs were extremely good, it is believed that the results obtained would be accurate.

3. ANN based correlation

Once optimum network architecture is found, the weights and biases are used to develop the ANN based correlation. The correlation estimates Q_{cr} in terms of seven input variables $(p, t, x, g, l, \sigma, d)$ as indicated before. Each input variable X is scaled up or normalized to the range {0:1} with its mean and standard deviation as:

$$X_{\text{scaleup}} = \frac{X - \overline{X}}{S} \tag{9}$$

where:

$$\overline{X} = \text{mean\_}X = \frac{\sum \overline{X}}{n} \tag{10}$$

$$S = \text{Std\_}X = \frac{\sum (X - \overline{X})^2}{(n-1)} \tag{11}$$

with reference to Eqs. (2) and (3) the ANN based correlation can be expressed as follows.

The values of hidden layer neurons are:

$$\begin{aligned} Z_1^2 &= \left(w_{11}^2 \times P + w_{12}^2 \times T + w_{13}^2 \times X + w_{14}^2 \times G + w_{15}^2 \times L + w_{16}^2 \times \delta + w_{17}^2 \times D + b_1^2\right) \\ Z_2^2 &= \left(w_{21}^2 \times P + w_{22}^2 \times T + w_{23}^2 \times X + w_{24}^2 \times G + w_{25}^2 \times L + w_{26}^2 \times \delta + w_{27}^2 \times D + b_2^2\right) \\ &\vdots \\ Z_9^2 &= \left(w_{91}^2 \times P + w_{92}^2 \times T + w_{93}^2 \times X + w_{94}^2 \times G + w_{95}^2 \times L + w_{96}^2 \times \delta + w_{97}^2 \times D + b_9^2\right) \end{aligned} \tag{12}$$

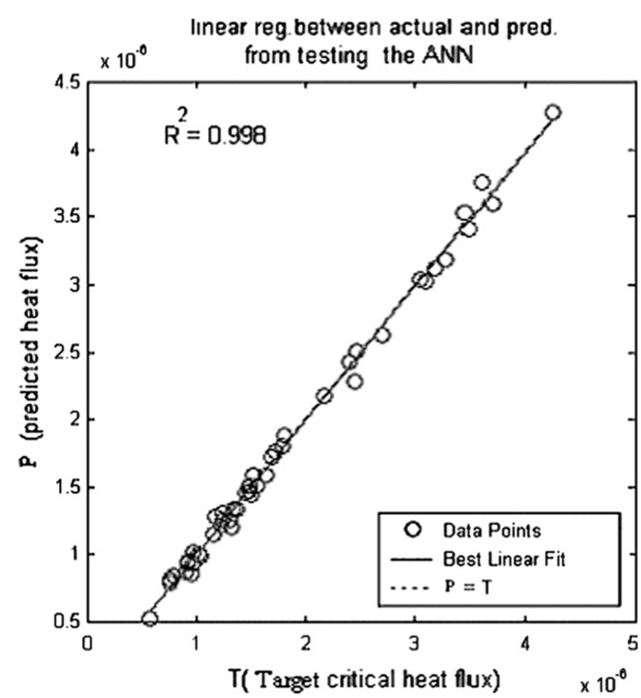

Fig. 4. Comparison of target and ANN-predicted values for critical heat flux (from testing process).

Using Eq. (6) and the above equations the functions $f_1^2, f_2^2, f_3^2, \ldots, f_9^2$ can be obtained.

Similarly, the weighted sum and biases of the output layers can be written as:

$$\begin{aligned} Z_1^3 = \Big(& w_{11}^3 \times f_1^2 + w_{12}^3 \times f_2^2 + w_{13}^3 \times f_3^2 + w_{14}^3 \times f_4^2 + w_{15}^3 \times f_5^2 \\ & + w_{16}^3 \times f_6^2 + w_{17}^3 \times f_7^2 + w_{18}^3 \times f_8^2 + w_{19}^3 \times f_9^2 + b_1^3\Big) \end{aligned} \tag{13}$$

From Eqs. (7) and (13) the required Q_{cr} can be obtained after converting the normalized critical heat flux to un-normalized one (using Eq. (9), after calculating S and $\overline{X}$ for Q_{cr} from the training target data).

Table 2 shows the scaled up parameters for the different given variables. And the different weights w_{jk}^i and biases b_j^i for the developed ANN based correlation are shown in Tables 3a and b.

In the developed ANN based correlation, the coefficient of the input parameters are used to evaluate the summation function of neuron j (Z_j^i) and the activation function of neuron f_j^i. These coefficients represent the weight and bias values of the summation function of each neuron belonging to the hidden layer of the trained network (Table 3a). For this purpose, nine equations are developed as the neural network model has nine hidden neurons (Eq. (12)). As well as nine log-sigmoid activation functions as shown by function (6). In the output neuron, only one summation function is used as only one output parameter exists which corresponds to Q_{cr} (Eq. (13)).

Table 1
Comparison between actual (experimental) Q_{cr} with that obtained by correlation (1) and ANN based correlation.

p (atm)	t (°C)	x	g (kg/m^2 h $\times 10^{-6}$)	l (mm)	δ (mm)	d (mm)	Q_{cr} exper. (kcal/m^2 h) $\times 10^{-6}$	Q_{cr} ANN. (kcal/m^2 h) $\times 10^{-6}$	Q_{cr} Eq. (1) (kcal/m^2 h) $\times 10^{-6}$	% ANN error[a]	%Correl. error[a]
100	232	0.004	7	400	0.75	10	3.59	3.68	4.3	−2.507	16.1
100	262.5	0.006	17.1	660	0.75	10	3.45	3.44	3.17	0.289	−8.75
100	105.5	0.198	3.6	565	1	10	3.7	3.81	2.96	−2.97	−7.3
100	301.5	0.292	6.5	890	1	10	1.51	1.49	1.37	1.325	−9.97
120	252	0	17.95	1000	0.75	10	3.48	3.49	3.58	−0.287	2.79
120	140	0.103	3.6	565	1	10	3.05	3.0	2.54	1.639	−20.02
120	273.5	0.104	14.5	1650	1	10	1.69	1.686	1.93	0.237	12.48
120	282	0.196	8.78	1650	1	10	1.17	1.2	1.29	−2.564	9.29
140	283	0.005	7.98	520	0.75	10	2.47	2.52	2.64	−2.024	6.5
140	306	0.1	11	890	0.75	10	1.72	1.78	1.93	−3.488	10.7
140	332	0.193	7.92	893	1	10	0.98	1	1.13	−2.041	13
140	283	0.335	3.31	1200	1	10	0.9	0.93	0.69	−3.333	−29.7
160	309.5	0	13.9	660	0.75	10	2.7	2.67	3.06	1.111	11.81
160	283	0.11	5.82	890	1	10	1.495	1.49	1.4	0.334	−6.8
160	330	0.19	3.6	565	1	10	0.93	0.98	0.85	−5.376	−9.9
160	335	0.233	10.27	1645	1	10	0.92	0.93	1.09	−1.087	15.88
180	313	0.018	19.3	1300	0.75	10	2.45	2.47	2.37	−1.633	−7.2
180	265	0.055	10.35	1650	1	10	1.81	1.82	1.87	−0.553	3.2
180	192	0.141	2.7	1650	1	10	0.755	0.76	0.775	−0.662	2.6
180	223.5	0.264	2.14	1650	1	10	0.58	0.565	0.48	2.586	−21.5
200	279	0.055	6.63	1650	1	10	1.15	1.13	1.03	1.739	−11.14
200	323.5	0.101	11.7	1650	1	10	1.34	1.36	1.27	−1.493	−5.16
200	341	0.208	10	1650	1	10	1.025	1.01	0.96	1.463	−6.5
200	361	0.334	13.15	1645	1	10	0.97	0.93	0.84	4.124	−15.6

[a] Percentage error = (difference/experimental Q_{cr}) × 100.

Table 2
Scale up parameters for different variables.

Variable (X)	S	$\bar{X}$
p	34.90963	148.250
t	49.30193	285.492
x	0.10273	0.14969
g	4.49061×10^6	9.8941×10^6
l	457.9942	1226.729
δ	0.9242	0.959375
d	0.129099	9.99167
Q_{cr}	8.01965×10^5	1.75091×10^6

4. Conclusion

The capability to predict the CHF is of vital importance to the safety of flow boiling processes. Various authors have established different techniques and different relationships for the prediction of CHF. The quantitative relationship between the main variables, however, varies from one author to another. The CHF prediction can be realized either by the table method or by best-fit method. Modern computational capabilities and numerical optimization techniques have limited the above two methods. ANN alternative techniques are accepted way to tackle complex and ill-defined problems. ANNs are able to learn key information patterns within a multi-information domain. Therefore, it is used as

Table 3a
Weights (w^i_{jk}) and biases (b^i_j) for the hidden layer.

Second layer ($i = 2$)								
w^i_{jk}, k								b^i_j
j	1	2	3	4	5	6	7	
1	−0.1956	−0.0166	0.2096	0.4115	−0.0660	−1.8571	−0.4553	0.2937
2	−2.0750	−0.6912	1.7181	−0.2923	−0.9223	2.2153	−0.0084	1.9344
3	−1.9971	−0.6494	1.6884	−0.3334	−0.7284	1.6143	0.1594	1.9595
4	−2.1942	0.8632	−1.8405	−1.0306	−1.898	0.9096	0.484	1.1489
5	0.1459	0.1924	−0.1856	−0.1351	0.0371	1.8357	0.1191	1.6052
6	0.1463	0.2844	−0.1979	−0.1652	0.1031	1.5721	−0.0253	1.8265
7	0.1940	−0.0575	−0.1926	−0.4514	0.0656	−2.4797	0.0213	1.7267
8	−2.6728	1.1927	−0.7879	0.0268	1.5786	−1.1333	0.0675	−4.7763
9	2.4236	−0.3670	−0.3041	1.5045	−0.6759	1.1543	−0.1257	3.7093

Table 3b
Weights (w^i_{jk}) and biases (b^i_j) for the output layer.

Third layer ($i = 3$)										
j	w^i_{jk}, k									b^i_j
	1	2	3	4	5	6	7	8	9	
1	184.748	6.8942	−6.7705	−0.9454	346.4331	−161.8427	149.9146	2.1724	−2.5602	−330.9704

a predictor of CHF based on the available database without knowing their best-fit correlations due to ANNs black-box characteristics. The developed ANN is applied to develop an ANN based correlation for estimating the CHF (*Q*cr) for flow of steam–water mixtures through pipes. The feed forward neural network (using the back propagation (BP) technique) is used in this study. Some statistical methods, such as the root-mean square (MSE) and the correlation coefficient (R^2) are applied. The optimum network parameters are obtained after many trials. These parameters include the learning rate of 0.75, momentum coefficient of 0.85 and the neuron number at hidden layer is 9. Therefore, the configuration 7–9–1 is the most optimal topology for this problem. The proposed ANN model structure (with nine neurons in the hidden layer) is capable of predicting the target Q_{cr}. Experimental results of Q_{cr} are compared with both the results obtained by the developed ANN based correlation and a best-fit correlation. Deviations between the results are found to be less than 5.5% and 30%, respectively.

The use of the developed formula, which can be employed with any programming language or spreadsheet program for estimating Q_{cr}, as described in this paper, may make the use of dedicated ANN software unnecessary to carry out in each training time. An advantage of the method is the straight forward modeling (with no loops) that can easily be incorporated into any programming language or spreadsheet. Also, as more experimental data are available in the future, these can be used to enrich the training database and return the networks in order to increase the prediction accuracy and possibly extend the range of applicability of the model.

References

[1] L.S. Tong, Y.S. Tang, in: Boiling Heat Transfer and Two Phase Flow, second ed. Taylor and Francis, London, 1997.
[2] C.H. Lee, I. Mudawar, A mechanistic critical heat flux model for subcoold flow boiling, Int. J. Heat Mass Transfer 14 (1988) 711–728.
[3] Y.A. Katto, A prediction model of subcooled water flow boiling for pressure in the range 0.1–20 MPa, Int. J. Heat Mass Transfer 35 (5) (1992) 1115–1123.
[4] K. Katto, Critical heat flux, Int. J. Multiphase Flow 20 (Suppl.) (1994) 53–90.
[5] Y.l. Kim, W.P. Baek, S.H. Chang, Critical heat flux under flow oscillation of water at low pressure, low flow conditions, Nucl. Eng. Des. 193 (1999) 131–143.
[6] G.F. Hewit, Critical heat flux in flow boiling, in: J.T. Rogers (Ed.), Proceedings of Sixth International Heat Transfer Conference, August 7–11, Toronto, Canada, vol. 6, 1978, pp. 143–180.
[7] D. David, I. Mudawar, Critical heat flux (CHF) for water flow in tubes I. Comparison and assessment of world CHF data, Int. J. Heat Mass Transfer 43 (2000) 2573–2604.
[8] D. David, I. Mudawar, Critical heat flux (CHF) for water flow in tubes II. Subcooled CHF correlations, Int. J. Heat Mass Transfer 43 (2000) 2605–2640.
[9] V.P. Bobkov, P.L. Kirillov, I.P. Smogalev, V.N. Vinogradov, Look-up table developing methods for critical heat flux in rod bundles, in: Proceedings of the Eighth International Topical Meeting on Nuclear Reactor Thermal-hydraulics (NURETH-8), Kyoto Japan (September 30–October 4, 1997) 1581–1589.
[10] D.C. Groeneveld, S.C. Cheng, T. Dean, 1986 AECL-UO critical heat flux look-up table, Heat Transfers Eng. 7 (1986) 46–62.
[11] P.S. Curtiss, M.J. Brandemuehl, J.F. Kreider, Energy management in central HVAC plants using neural networks, in: J.S. Haberl, R.M. Nelson, C.C. Culp (Eds.), Central HVAC Plants using Neural Networks, The Use of Artificial Intelligence in Building Systems, ASHRAE, 1995, pp. 199–216.
[12] A.H. Kah, Q.Y. San, S.C. Guan, W.C. Kiat, Y.C. Koh, Smart air-conditioning system using multiplayer perception neural network with a modular approach, , In: Proceedings of the IEEE International Conference ICNN'95, Perth, Western Australia, vol. 5 (1995) 2314–2319.
[13] J.F. Kreider, X.A. Wang, Artificial neural network demonstration for automated generation of energy use predictions for commercial buildings, in: J.S. Haberl, R.M. Nelson, C.C. Culp (Eds.), The Use of Artificial Intelligence in Building Systems, ASHRAE, 1995, pp. 193–198.
[14] S. Kalogirou, Long-term performance prediction of forced circulation solar domestic water heating systems using artificial neural networks, Applied Energy 66 (1) (2000) 63–74.
[15] S. Kalogirou, M. Bojic, Artificial neural networks for the prediction of the energy consumption of a passive solar building, Energy Int. J. 25 (5) (2000) 479–491.
[16] O.L. Peskov, V.I. Subbotin, B.A. Zenkevich, N.D. Sergeyev, The Critical Heat Flux for the Flow of Steam–Water Mixtures through Pipes, in the Symposium of "Problems of Heat Transfer and Hydraulics of Two-phase Media", Pergamon Press, Kutateladze, 1969.
[17] S.A. Kalogirou, Applications of artificial neural-networks for energy systems, Appl. Energy 67 (2000) 17–35.
[18] S. Haykin, Neural Networks, A Comprehensive Foundation, New Jersey, 1994.
[19] G.E. Nasr, E.A. Badr, C. Joun, Back propagation neural networks for modeling gasoline consumption, Energy Convers. Manage. 44 (2003) 893–905.
[20] S. Sreekanth, H.S. Ramaswamy, S.S. Sablani, S.O. Prasher, A neural network approach for evaluation of surface heat transfer coefficient, J. Food Process. Preserve 23 (1999) 329–348.
[21] V. Kurkova, Kolmogorov's theorem and multilayer neural networks, Neural Netw. 5 (1992) 501–506.
[22] Y. Ito, Approximation capabilities of layered neural networks with sigmoid units on two layers, Neural Comput. 6 (1994) 1233–1243.
[23] Matlab Version 7.0 Online Manual.
[24] A. Palau, E. Velo, L. Puigianer, Use of neural networks and expert systems to control a gas/solid sorption chilling machine, Int. J. Refrig. 22 (1999) 59–66.